Original Article

Indole-3-pyruvic acid alleviates rheumatoid arthritis via the aryl hydrocarbon receptor pathway

Tai Huang[1], Lin Cheng[1], Yan Jiang[1], Lingling Zhang[2,3], Long Qian[1,3]

[1]Department of Rheumatology and Immunology, The Second Affiliated Hospital of Anhui Medical University, Hefei, China; [2]Institute of Clinical Pharmacology, Anhui Medical University, Hefei, China; [3]Rheumatoid Arthritis Research Center, Anhui Medical University, Hefei, China

Contributions: (I) Conception and design: L Qian, L Zhang, T Huang; (II) Administrative support: L Qian; (III) Provision of study materials or patients: L Qian, L Cheng, T Huang, Y Jiang; (IV) Collection and assembly of data: T Huang, L Cheng, Y Jiang; (V) Data analysis and interpretation: All authors; (VI) Manuscript writing: All authors; (VII) Final approval of manuscript: All authors.

Correspondence to: Long Qian. Department of Rheumatology and Immunology, The Second Affiliated Hospital of Anhui Medical University, 678 Furong Road, Economic and Technological Development Zone, Hefei, China. Email: Longqian0551@163.com. Lingling Zhang. Institute of Clinical Pharmacology, Anhui Medical University, 81 Meishan Road, Shushan District, Hefei, China. Email: ll-zhang@hotmail.com.

Background: In previous studies, we found that smoking may participate in the pathogenesis of rheumatoid arthritis (RA) via the aryl hydrocarbon receptor (AhR) pathway. However, when we conducted a subgroup analysis, the expression of AhR and CYP1A1 in healthy people was higher than that in RA patients. We considered that endogenous AhR ligands may exist *in vivo* that activate AhR to play a protective role. Indole-3-pyruvic acid (IPA) is a tryptophan (Trp) metabolite produced by the indole pathway and serves as a ligand of AhR. This study aimed to reveal the effect and mechanism of IPA in RA.

Methods: A total of 14 patients with RA and 14 healthy volunteers were enrolled. The differential metabolites were screened with liquid chromatography-mass spectrometry (LC-MS) metabolomics technology. We also treated peripheral blood mononuclear cells (PBMCs) with IPA to evaluate the effect on the differentiation of T helper 17 (Th17) cells or regulatory T (Treg) cells. To determine whether IPA can be used to alleviate RA, we administered IPA to rats with collagen-induced arthritis (CIA). Methotrexate was used as a standard drug for CIA.

Results: When the dose reached 20 mg/kg/d, the severity of CIA was significantly reduced. *In vitro* experiments verified that IPA inhibited the differentiation of Th17 cells and promoted the differentiation of Treg cells, but this effect was weakened by CH223191.

Conclusions: IPA is a protective factor for RA; it can restore the Th17/Treg cell balance through the AhR pathway, which can alleviate RA.

Keywords: Indole-3-pyruvic acid (IPA); Th17 cell; Treg cell; aryl hydrocarbon receptor (AhR); rheumatoid arthritis (RA)

Submitted Jan 28, 2023. Accepted for publication Mar 13, 2023. Published online Mar 15, 2023.
doi: 10.21037/atm-23-1074
View this article at: https://dx.doi.org/10.21037/atm-23-1074

Introduction

Rheumatoid arthritis (RA) is a chronic inflammatory joint disease that can lead to cartilage and bone damage and disability (1). It is characterized by a close interaction between cells of the innate immune system and the adaptive immune system. It is well known that this interaction leads to the development of local and systemic inflammation at different stages of the disease (2). $CD4^+$ T helper (Th) cells play an important role in the development of RA by regulating the adaptive immune response. Th17 cells, which form the main subgroup of $CD4^+$ Th cells, can produce large numbers of marker cytokines and participate in host defense and immune homeostasis. In RA patients,

Notch signaling is upregulated, and there are changes in the expression patterns of Notch signaling in helper T cells. Notch signaling plays a role in regulating the function of Th17 cells by integrating signals provided by cytokines such as IL-6 or TGF-β (3). In addition, the plasticity and pathogenicity of Th17 cells are closely related to the disease activity of RA (4). Regulatory T (Treg) cells are important components of peripheral immune tolerance, and Treg dysfunction is a potential mechanism that leads to the destruction of self-tolerance in RA progression (5). Disturbance of the Th17/Treg cells balance in peripheral blood plays an important role in the development of RA (6).

Aryl hydrocarbon receptor (AhR) is a transcription factor that is widely expressed in various tissues and cells, especially immune cells (7). AhR is known to play a significant role in the activation and proliferation of Th17 cells. When AhR is activated by polycyclic aromatic hydrocarbons present in particulate matter, it enhances the proliferation and differentiation of Th17 cells, as well as their ability to produce proinflammatory cytokines, which can contribute to the development of RA (8). However, when AhR is activated, the diversity of ligands may lead to different effects on Th17 cells. When other kinds of ligands, such as tetrachlorodibenzo-p-dioxin (TCDD), stimulate AhR, they can inhibit the differentiation of Th17 cells. A previous study has found that smoking may contribute to the pathogenesis of RA through the AhR pathway (9). However, through subgroup analysis, we have found that the levels of AhR and its downstream target gene *CYP1A1* are higher in nonsmoking healthy people than in nonsmoking RA patients. Therefore, we hypothesized that some endogenous substances could play a protective role in RA by activating AhR *in vivo*. Previous research has shown that AhR can directly control the expression of *Foxp3* and participate in the differentiation of Treg cells. AhR affects the differentiation of Th17 cells and Treg cells in the opposite way (10). AhR is regarded as a critical factor in the immune response, and its role in various immune mechanisms has been extensively studied, providing a deeper understanding of the molecular mechanisms involved in immune-inflammatory diseases such as RA. Consequently, AhR has emerged as a promising therapeutic target for the treatment of RA (11).

Tryptophan (Trp) is an essential aromatic amino acid obtained by humans through dietary intake. Common sources of dietary Trp are fish, poultry, grains, and dairy products (12). The intestine is the main location of Trp metabolism. Dietary Trp is processed by 3 main metabolic pathways: (I) the uridine pathway through indoleamine 2,3-dioxygenase 1, which mainly occurs in immune cells and epithelial cells; (II) the 5-hydroxytryptamine pathway of Trp hydroxylase 1 in intestinal chromaffin cells; and (III) the intestinal microbiota directly converts Trp into several molecules, including AhR ligands (13). It has been reported that Trp catabolites affect the differentiation of $CD4^+$ T helper cells into Treg cells and Th17 cells through AhR (14). The Th17/Treg cells balance plays an important role in autoimmune and inflammatory diseases (15). In addition, it has been found that indole-3-pyruvic acid (IPA), through symbiotic bacteria, improves the health of a series of different organisms in an AhR-dependent manner (16). We hypothesized that Trp metabolites decomposed by AhR may alleviate the severity of disease and promote health. We present the following article in accordance with the ARRIVE reporting checklist (available at https://atm.amegroups.com/article/view/10.21037/atm-23-1074/rc).

Highlight box

Key findings

- IPA is a protective factor for RA and can alleviate RA.

What is known and what is new?

- Previous studies have found that smoking may contribute to the pathogenesis of RA through the AHR pathway.
- We first analyzed the plasma of nonsmoking RA patients and nonsmoking healthy volunteers based on LC/MS metabonomics technology, found that the Trp metabolic pathway played an important role. We also screened IPA as a potential biomarker of RA.

What is the implication, and what should change now?

- Researchers need to consider the relationship between intestinal flora and metabolites.

Methods

Participants

The RA patients enrolled in this study were recruited by the Second Affiliated Hospital of Anhui Medical University and fulfilled the 2010 American College of Rheumatology/European League Against Rheumatism (ACR/EULAR) criteria for the classification of RA (17), as did the sex- and age-matched healthy volunteers. Disease activity was evaluated using the Disease Activity Score based on 28 joints (DAS28). All participants provided informed

consent. The exclusion criteria were as follows: (I) the presence of diarrhea, diabetes, ulcerative colitis, Crohn's disease, or other infectious diseases; (II) smoking, reception of chemotherapy, radiotherapy, surgery, or disease-modifying antirheumatic drug treatment; (III) reception of antibiotics, hormones, Chinese herbal medicine, or probiotics within the last 6 months; (IV) significant changes in diet 1 week before sampling; (V) currently in a state of pregnancy, lactation, or menstruation; (VI) complications with the respiratory system, digestive system, endocrine system, or blood system; other diseases; or serious heart, liver, or kidney damage; (VII) other chronic diseases including diabetes, coronary heart disease, and tumors; (VIII) complications with other rheumatic diseases; and (IX) serious complications. This study was conducted in accordance with the Declaration of Helsinki (as revised in 2013), and the protocol was approved by the Ethics Committee of The Second Affiliated Hospital of Anhui Medical University (No. YX2021-131).

Metabolomics analysis

Metabolomics analyses were performed based on the liquid chromatography-mass spectrometry (LC-MS) method by Majorbio Ltd. (Shanghai, China).

Plasma separation

The blood was collected with an ethylenediaminetetraacetic acid (EDTA) anticoagulant tube, transferred into an enzyme-free EP tube, and centrifuged at 3,000 rpm at 4 ℃ for 10 minutes. The upper layer of pale-yellow liquid, namely, the plasma, was aspirated and placed into an RNase-free cryopreservation tube. The samples were wrapped with tin foil, immediately frozen in liquid nitrogen for 30 minutes, and then transferred to a –80 ℃ freezer for storage.

Metabolite extraction

A 100 µL liquid sample was accurately weighed, and the metabolites were extracted using 400 µL of a methanol:water (4:1, v/v) solution. The resulting mixture was allowed to settle at –20 ℃, then treated with a high-throughput tissue crusher (Wonbio-96c; Shanghai Wanbo Biotechnology Co., Ltd., Shanghai, China) at 50 Hz for 6 minutes, vortexed for 30 seconds, and ultrasonicated at 40 kHz for 30 minutes at 5 ℃. The samples were subsequently placed at –20 ℃ for 30 minutes to precipitate proteins. After centrifugation at 13,000×g at 4 ℃ for 15 minutes, the resulting supernatant was carefully transferred to sample vials for LC-MS/MS analysis.

Quality control (QC) sample

A pooled QC sample was prepared by mixing equal volumes of all the samples. The QC samples were processed and analyzed in the same manner as the individual samples. The QC sample was injected at regular intervals (every 8 samples) to monitor the stability of the analysis.

Ultrahigh performance liquid chromatography-MS/MS analysis

LC/MS analysis was performed using a Q Exactive HF mass spectrometer coupled to a Vanquish Horizon UHPLC system (Thermo Fisher Scientific, Waltham, MA, USA) equipped with an ACQUITY UPLC HSS T3 column (100 mm × 2.1 mm i.d., 1.8 µm; Waters, Milford, MA, USA). The mobile phases consisted of 0.1% formic acid in water with formic acid (0.1%) (solvent A) and 0.1% formic acid in acetonitrile:isopropanol (1:1, v/v) (solvent B). The solvent gradient was changed according to the following conditions (Table S1). The sample injection volume was 2 µL, and the flow rate was set to 0.4 mL/min. The column temperature was maintained at 40 ℃. Mass spectra were recorded in positive and negative ion modes using electrospray ionization. The specific parameters can be found in Table S2.

Data preprocessing and annotation

The Progenesis QI 2.3 software (Nonlinear Dynamics; Waters) was used for peak detection and alignment of the raw data. The resulting data matrix contained information on retention time (RT), mass-to-charge ratio (m/z) values, and peak intensity. Metabolic features that were detected in at least 80% of any set of samples were retained after filtering, and minimum metabolite values were imputed for specific samples where the levels of metabolites were below the limit of quantification. Each metabolic feature was normalized by sum, and the internal standard was used for data quality control (reproducibility). Metabolic features with a relative standard deviation (RSD) of QC >30% were discarded. After normalization and imputation, log10-transformed data were statistically analyzed to identify significant differences in metabolite levels between comparable groups. The mass spectra of these metabolic features were identified using accurate mass, MS/MS fragment spectra, and isotope ratio differences by searching reliable biochemical databases, such as the Human

Metabolome Database (HMDB; http://www.hmdb.ca/) and Metlin database (https://metlin.scripps.edu/).

Multivariate statistical analysis

A multivariate statistical analysis was performed using the ropls (version 1.6.2; http://bioconductor.org/packages/release/bioc/html/ropls.html) R package from Bioconductor on the Majorbio Cloud Platform (https://cloud.majorbio.com). Orthogonal partial least squares discriminant analysis (OPLS-DA) models were used to analyze the data, and a permutation test with a permutation number of 200 was used to validate the OPLS-DA models. The p-values were estimated with paired Student's *t*-tests on single-dimensional statistical analysis. Statistically significant differences among groups were selected with a variable importance of projection (VIP) value greater than 1 and a p-value less than 0.05. Both the Kyoto Encyclopedia of Genes and Genomes (KEGG; https://www.kegg.jp/kegg/pathway.html) pathway database and Metabolon (https://www.metabolon.com/) -provided annotations were used to map metabolites to pathways. Pathway enrichment analysis was performed with the Python software package scipy.stats, and the biological pathway most relevant to the experimental treatment was obtained through Fisher's exact test.

Cell culture

Peripheral blood mononuclear cells (PBMCs) were isolated from fresh blood of healthy donors by Ficoll density gradient centrifugation (18). Living human PBMCs were inoculated at 10^6 cells/mL with T Cell Expansion Medium (10981; STEMCELL Technologies, Vancouver, BC, Canada). Then, 20 µl/mL of CD3/CD28 T Cell Activator (10971, STEMCELL) was used to stimulate PBMCs and added to the cell suspension. Next, 10 ng/mL rHuIL-1 (GMP-101-01B; PrimeGene, Shanghai, China), 10 ng/mL hIL-6 (GMP-101-06, PrimeGene), 1 ng/mL hTGF-β (105-49, PrimeGene), 5 µg/mL anti-IFN-γ (14-7318-81; eBioscience; San Diego, CA, USA) and 5 µg anti-IL-4 (14-7049-81, eBioscience) were used for the differentiation of Th17 cells, and 10 ng/mL IL-2 (GMP-101-02, PrimeGene), 1 ng/mL TGF-β, 5 µg/mL anti-IFN-γ, and 5 µg anti-IL-4 were used for the differentiation of Treg cells. The AhR agonist 6-Formylindolo[3,2-b]carbazole (FICZ; 100 nM) was used as a positive control. CH223191 was added at a final concentration of 10 nM to inhibit AhR. To detect the effect of IPA on the differentiation of Th17 cells through AhR, we seeded PBMCs in 48-well plates and assigned them to 1 of the following groups: the control group, which received 20 µL/mL CD3/CD28 T Cell Activator; the Th17 group, which received the same treatment as the control group plus 10 ng/mL rHuIL-1, 10 ng/mL hIL-6, 1 ng/mL hTGF-β, 5 µg/mL anti-IFN-γ, and 5 µg anti-IL-4; the IPA group, which received the same treatment as the Th17 group plus 500 µM IPA; the CH223191 group, which received the same treatment as the Th17 group plus 10 nM CH223191; and the IPA + CH223191 group, which received the same treatment as the IPA group plus 10 nM CH223191. The treatment protocols to detect the effect of IPA on the differentiation of Treg cells through AhR were as follows: the control group received 20 µL/mL CD3/CD28 T Cell Activator, the Treg group received the same treatment as the control group plus 10 ng/mL IL-2, 1 ng/mL TGF-β, 5 µg/mL anti-IFN-γ, and 5 µg anti-IL-4; the IPA group received the same treatment as the Treg group plus 500 µM IPA; the CH223191 group received the same treatment as the Treg group plus 10 nM CH223191; and the IPA + CH223191 group received the same treatment as the IPA group plus 10 nM CH223191.

Cell viability determination by Cell Counting Kit-8 (CCK-8) assay

A proper amount of cells was added to complete ImmunoCult™-XF T-cell expansion solution (STEMCELL), and the cell density of each group was 10^5. After the cell suspension was prepared, it was gently mixed and inoculated into a 48-well plate. Then, it was incubated with IPA at different concentrations (0, 1, 5, 10, 25, 50, 100, 250 and 500 µM) at 37 ℃ and 5% CO_2 for 24, 48, and 72 hours. After culturing to different time points, 10 µL of CCK-8 was added to each well, and the cells were cultured for 1 hour. Finally, the absorbance value [optical density (OD)450 value] of each well was measured at 450 nm by enzyme-linked immunosorbent assay (ELISA).

Animals

All 6- to 7-week-old male Sprague–Dawley (SD) rats were purchased from Speyford (Beijing) Biotechnology Co., Ltd. (Experimental animal license: SCXK [Beijing] 2019-0010) and weighed 180–240 g. The rats were randomly assigned to each group, and there was no significant difference in weight. All experimental animals were raised in the animal room of the Institute of Clinical Pharmacology, Anhui Medical University. The temperature was set at 25±1 ℃, the humidity was controlled at 40–70%, and the light/dark cycle

was maintained every 12 hours. All rats were able to freely eat and drink and had enough space for activities. The rats were euthanized 24 hours after the last dose and after CO_2 narcosis by cervical dislocation followed by exsanguination. The animal study protocol in this study was approved by the Experimental Animal Ethics Committee of the Institute of Clinical Pharmacology of Anhui Medical University (No. PZ-2022-22), in compliance with Anhui Medical University guidelines for the care and use of animals.

Animal modelling and drug administration

Collagen-induced arthritis (CIA) was induced as previously described. That is, bovine type II collagen (2 mg/mL; Chondrex, Woodinville, WA, USA) and complete Freund's adjuvant (5 mg/mL, Chondrex) were mixed at a ratio of 1:1 to form an emulsion. Based on previous research (19), we chose a dose of 20 mg/kg for IPA *in vivo*. The dose of 10 mg/kg was selected as a comparative observation to evaluate whether the effect of IPA on CIA is dose-dependent. The SD rats were randomly divided into the following groups (6 rats per group): the control group, CIA group, methotrexate (MTX) group, IPA-10 (10 mg/kg) group, IPA-20 (20 mg/kg) group, CH223191 group, and CH223191 + IPA group. The rats in the CIA, MTX IPA-10, IPA-20, CH223191, and CH223191 + IPA groups were injected with 0.1 mL of emulsion in the tail and 0.15 mL of emulsion in the back (3 inoculation sites were chosen on the central axis of the back of rats, and 50 μL of immunological emulsion was inoculated into each inoculation site). After 7 days, the second immunization was carried out according to the injection plan, and the injection point was different from the first immunization point. Drug administration was initiated on day 8. We decided that IPA was to be intragastrically (i.g.) administered at 20 mg/kg/d in the IPA-20 group CH223191 + IPA groups, and 10 mg/kg/d in the IPA-10 group. The rats in the MTX group were administered MTX (1.5 mg/kg i.g. twice a week) (20). CH223191 was intraperitoneally administered at 10 mg/kg/d (21) in the CH223191 and CH223191 + IPA groups. The control group was injected with a comparable volume of solvent. The severity of the disease was evaluated by the clinical arthritis score. Each paw was scored by visual inspection, with the score ranging from 0 to 4, as follows: 0 = normal paw; 1 = ankle or wrist mildly swollen (definite redness and swelling); 2 = ankle or wrist moderately red and swollen; 3 = entire paw including digits severely red and swollen; 4 = limb maximally inflamed involving multiple joints.

Molecular docking

AutodockVina software was used for performing molecular docking studies, which predicts the binding affinity and mode of interaction between a protein and a ligand (22). In this study, we analyze the binding affinities and modes of interaction between IPA and AhR. The molecular structures of IPA were obtained from PubChem Compound (https://pubchem.ncbi.nlm.nih.gov/) (23), and the 3D coordinates of AhR (PDB ID, 4M4X) were downloaded from the Protein Data Bank (PDB; http://www.rcsb.org/pdb/home/home.do). Both the protein and molecular files were converted into PDBQT format, and the grid box was centered to cover the domain of each protein and to accommodate free molecular movement. The grid box was set to 30 A×30 A×30 A, and grid point distance was 0.05 nm. The molecular docking studies were performed using Autodock Vina 1.2.2 (http://autodock.scripps.edu/).

Quantitative reverse transcription polymerase chain reaction assay

Total RNA was isolated from spleens and PBMCs by means of TRIzol Reagent (15596026; Ambion, Austin, TX, USA), and HiScript II Q RT SuperMix for qPCR kit (R222; Vazyme Biotech Co. Ltd, Nanjing, China) were used to generate complementary DNA (cDNA). SYBR Green quantitative polymerase chain reaction (qPCR) was performed on an Applied Biosystems™ QuantStudio™ 6 Flex real-time fluorescent polymerase chain reaction system (Applied Biosystems, Waltham, MA, USA) using a SYBR® Green PCR kit (22204, Tolo Biotech., Shanghai, China), cDNA, and primers for rat genes. The primer sequences (*Table 1*) were synthesized by Sangon Biotech Ltd. (Shanghai, China). The data were normalized to those of the reference gene β-*actin*, and the relative messenger RNA (mRNA) level was calculated by the $2^{-\Delta\Delta Ct}$ method.

Flow cytometry analysis

We collected PBMCs isolated from healthy humans and cell suspensions isolated from the spleens of the rats and incubated them with each fluorescently labelled monoclonal antibody at 4 ℃ for 30 minutes. The following monoclonal antibodies were used for flow cytometry analysis with a BD FACSCanto™ multicolour flow cytometer (Becton, Dickinson, and Co. [BD], Franklin Lakes, NJ, USA): Th17 cells: rat anti-CD4 (APC, 17-0040-80, eBioscience™),

Table 1 Primer sequences used for the qPCR assay

Gene	Forward primer (5'-3')	Reverse primer (5'-3')
β-actin (human)	CCTGGCACCCAGCACAAT	GGGCCGGACTCGTCATAC
β-actin (rat)	TGTCACCAACTGGGACGATA	GGGGTGTTGAAGGTCTCAAA
AhR (human)	GTCTCCCCCAGACAGTAGTC	CGACATATGAAGCACCTCTCCA
AhR (rat)	GGGTACACAGTTGGACTTCCC	AGCCCTTACCTTGCTTAGGAAC
CYP1A1 (human)	AAGGAGGCTGAGGTCCTGATA	TTCCAGAGCCAACCACCTCC
CYP1A1 (rat)	GTAGTTCTTGCAGCTTTCCCC	CAAGGCAGAATGTGGTGACG
RORγt (human)	GTGGGGACAAGTCGTCTGG	AGTGCTGGCATCGGTTTCG
RORγt (rat)	TCGTCCTCGTCAGAATGTGC	CAGGACGGTCCAAGGCTCG
Foxp3 (human)	GTGGCCCGGATGTGAGAAG	GGAGCCCTTGTCGGATGATG
Foxp3 (rat)	TCACACGCATGTTCGCCTACTTC	CTCACTCTCCACTCGCACAAAGC

qPCR, quantitative polymerase chain reaction.

human anti-CD4 (APC, E-AB-F1109E, eBioscience™), rat anti-IL-17 (PE, 12-7177-81, eBioscience™), and human anti-IL-17 (PE, 12-7179-42, eBioscience™); Treg cells: rat anti-CD4 (APC, 17-0040-80, eBioscience™), human anti-CD4 (APC, E-AB-F1109E, eBioscience™), rat anti-CD25 (PE, 12-0259-80, eBioscience™), human anti-CD25 (PE-Cyanine5.5, 35-5773-80, eBioscience™), rat anti-Foxp3 (PE-Cyanine5.5, 35-5773-80, eBioscience™), and human anti-Foxp3 (PE-Cyanine5.5, 35-4776-41, eBioscience™). The data were then analyzed with FlowJo 10.6.2 software (BD).

X-ray evaluation

Rats were anesthetized with 5% isoflurane, maintained via inhalation of 2% isoflurane, and then examined by X-ray to observe swelling of periarticular soft tissue, bone destruction, bone erosion, joint space stenosis, and joint damage.

Hematoxylin and eosin staining

After the rats were killed, the right hind limbs were placed in 10% neutral formalin solution for 10 days, and the liquid was changed every 3 days. The samples were decalcified with 10% EDTA solution for 2 months. The samples were then dehydrated, paraffin embedded, and sectioned. Hematoxylin and eosin (HE) staining was used to observe inflammatory cell infiltration and bone erosion. The following criteria were used to assess bone erosion: 0 = no swelling or bone damage, 1 = mild bone damage, 2 = moderate bone erosion, and 3 = severe bone erosion. For inflammation scoring, we assess the percentage of infiltrating mononuclear inflammatory cells, as follows: 0 = absent, 1 = mild (1–10%), 2 = moderate (11–50%), and 3 =severe (51–100%).

Measurement of cytokine concentrations

We measured the plasma or cell supernatant levels of TNF-α (rat: RX302058R), IL-1β (rat: RX302869R), IL-17A (rat: RX-G301875R), and IL-10 (rat: RX302880R) using ELISA kits. These kits were obtained from RUIXIN BIOTECH (Quanzhou, China). We performed all measurements in accordance with the manufacturer's instructions. Absorbance values were measured using a Varioskan LUX Multimode Microplate Reader (Thermo Fisher Scientific).

Statistical analysis

All data were analyzed using GraphPad Prism 8.0.1 software (GraphPad Software Inc., San Diego, CA, USA). These data are presented as the mean ± standard deviation (SD) unless otherwise stated. One-way analysis of variance (ANOVA) followed by Tukey's test was used to analyze multiple comparisons. For comparison of multiple groups of data with nonnormal distribution, Kruskal–Wallis one-way ANOVA on ranks was used. Spearman correlation analysis was used in our study. Statistical significance was set

Table 2 Demographic and clinical features of patients with rheumatoid arthritis and healthy participants

Variable	RA (n=14)	Control (n=14)
Male, n	0	0
Age (years), mean ± SD	55.40±14.37	50.64±17.56
Disease course (years), mean ± SD	5.27±7.64	–
Rheumatoid factor (IU/mL), mean ± SD	245.83±419.26	–
DAS28, mean ± SD	4.82±1.66	–

RA, rheumatoid arthritis; SD, standard deviation; DAS28, Disease Activity Score based on 28 joints.

at P<0.05.

Results

Characteristics of the study population

As shown in *Table 2*, age and sex were matched between patients with RA and controls.

Metabolomics results

LC-MS was used to detect the metabolites in plasma samples from 28 participants. The basic peak intensity diagram of QC samples in participants' plasma samples under positive and negative ion modes is shown in Figure S1. According to the analysis of the original LC-MS data, a total of 25,134 ion peaks were detected, among which 20,268 ion peaks remained after the filtration of RSD ≥30% and missing values ≥20% in the group. To better visualize the subtle similarities and differences between complex datasets, OPLS-DA was carried out. The OPLS-DA score plots (*Figure 1A*) showed that the clusters of the 2 groups were obviously separated. According to the OPLS-DA method dataset, the results showed that R^2Y (CUM) =0.925 and Q^2 (CUM) =0.741, suggesting that the OPLS-DA model is stable and has good predictive ability (*Figure 1B*). The fitting of the PLS-DA model was evaluated through 200 random permutation tests. The results showed that the intercept values of R^2 and Q^2 were 0.8318 and –0.3385, respectively, indicating that the model had no risk of overfitting (*Figure 1C*). Through comparison between the 2 groups, the number of ion peaks that met the difference screening conditions was 3,111, of which the number of identified differential metabolites with names was 126 (P<0.05, VIP value in OPLS-DA model analysis >1, difference multiple >1) (*Figure 1D*). We conducted KEGG pathway enrichment analysis for the 62 differential metabolites identified on the cloud platform and found that 5 metabolic pathways were involved in the occurrence of RA, including Trp metabolism, steroid hormone biosynthesis, primary bile acid biosynthesis, histidine metabolism, and unsaturated fatty acid biosynthesis (*Figure 1E*). Trp metabolism (impact value =0.221) was the main metabolic pathway. The heatmap showed that the differentially expressed metabolites of the Trp metabolism pathway exhibited a downward trend in RA patients. VIP analysis and random forest analysis showed that among the differentially expressed metabolites of the Trp metabolism pathway, the IPA value had the largest difference between the 2 groups, and the highest contribution was generated by the grouping (*Figure 1F,1G*). Then, the receiver operating characteristic (ROC) curve of IPA was analyzed, and its area under the curve (AUC) was 0.929 (95% CI: 0.841 to 1), with high diagnostic performance (*Figure 1H*).

Relationships between IPA and DAS28

In the RA group, IPA was mildly correlated with the DAS28 score (Spearman's r=–0.615, P=0.019) (*Figure 2*).

Impact of IPA on PBMCs

To evaluate the affinity of IPA for AhR, we performed molecular docking analysis. The results showed that IPA bound to AhR. For AhR, IPA had low binding energy of -7.383 kcal/mol, indicating highly stable binding (*Figure 3A*). We used CCK-8 assays to evaluate the effect of different concentrations of IPA on PBMC activity. When the IPA concentration was lower than 100 μM, the cell activity was lower than 90% (*Figure 3B*). Therefore, we chose 100, 250, and 500 μM for further processing. To investigate the effect of IPA on AhR in PBMCs, we treated PBMCs with IPA for 72 h. IPA can increase the expression of AhR mRNA. The mRNA expression of *CYP1A1*, a target gene downstream of AhR, was upregulated (*Figure 3C*).

Effect of IPA on the differentiation of Th17 cells through AhR

PBMCs activated with IPA significantly inhibited the differentiation of Th17 cells and the mRNA expression of

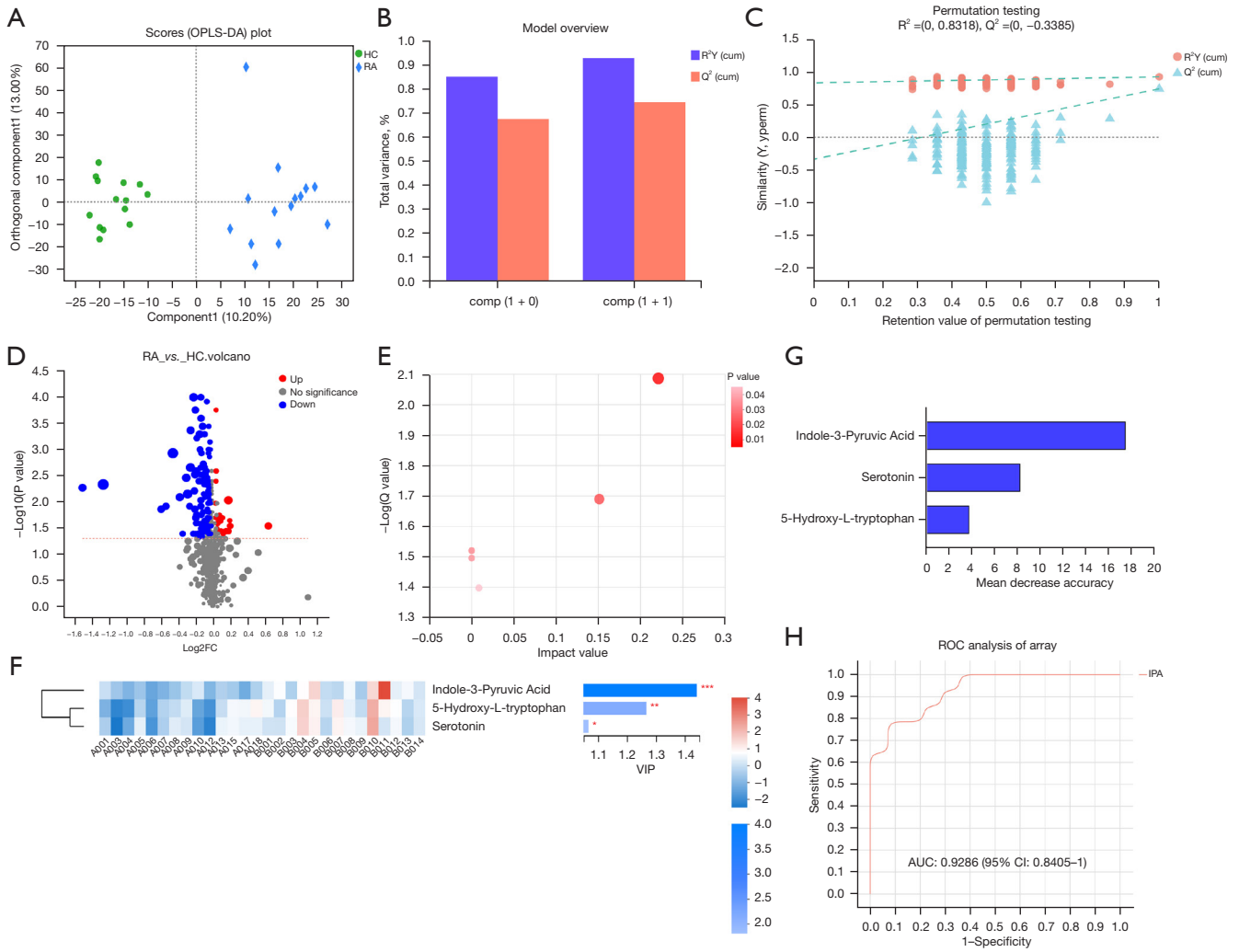

Figure 1 Metabolomics results. (A) OPLS-DA score plots. (B) OPLS-DA model overview. (C) A permutation test was performed to validate the OPLS-DA model. (D) Volcano plot of the differentially expressed metabolites. (E) KEGG pathway enrichment analysis of the most significantly changed pathways. (F) Heatmap and VIP analysis of the significantly altered metabolites of tryptophan metabolism pathway. (G) Random forest analysis for the differentially expressed metabolites in Trp metabolism. (H) ROC curve of IPA. *, P<0.05; **, P<0.01; ***, P<0.001. OPLS-DA, orthogonal partial least squares discriminant analysis; RA, rheumatoid arthritis group; HC, health control group; FC, fold change; KEGG, Kyoto Encyclopedia of Genes and Genomes; VIP, variable importance of projection; Trp, tryptophan; ROC, receiver operating characteristic; AUC, area under the ROC curve; IPA, indole-3-pyruvic acid.

the transcription factor RORγt. Notably, IPA was shown to promote the expression of CYP1A1 during Th17 differentiation. To study whether AhR contributes to the IPA-mediated inhibition of Th17 cell differentiation, naïve PBMCs were treated with CH223191 (an AhR antagonist) under IPA treatment. IPA significantly reduced the inhibition of *RORγt* mRNA expression (*Figure 4*).

Effect of IPA on the differentiation of Treg cells through AhR

To further reveal how IPA restores the balance between Th17 and Treg cells, we conducted the specific conditions *in vitro* experiment to observe the effect of IPA on the Treg differentiation of PBMCs. The results showed that

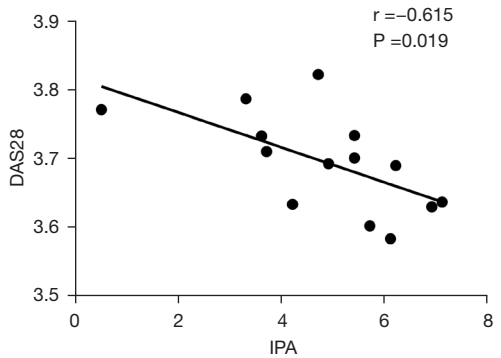

Figure 2 Relationships between IPA and DAS28. IPA, indole-3-pyruvic acid; DAS28, Disease Activity Score based on 28 joints.

IPA induced Treg cell differentiation and promoted the expression of the transcription factor Foxp3 and the cytokine IL-10. As IPA can promote CYP1A1 expression, we also studied the role of AhR in IPA-induced Treg cell differentiation. Our findings indicated that CH223191 inhibited the upregulation of IL-10 and *Foxp3* mRNA levels induced by IPA, suggesting that AhR plays a crucial role in Treg cell differentiation induced by IPA (*Figure 5*).

Effect of IPA in rats with CIA

In this experiment, MTX was used as the standard

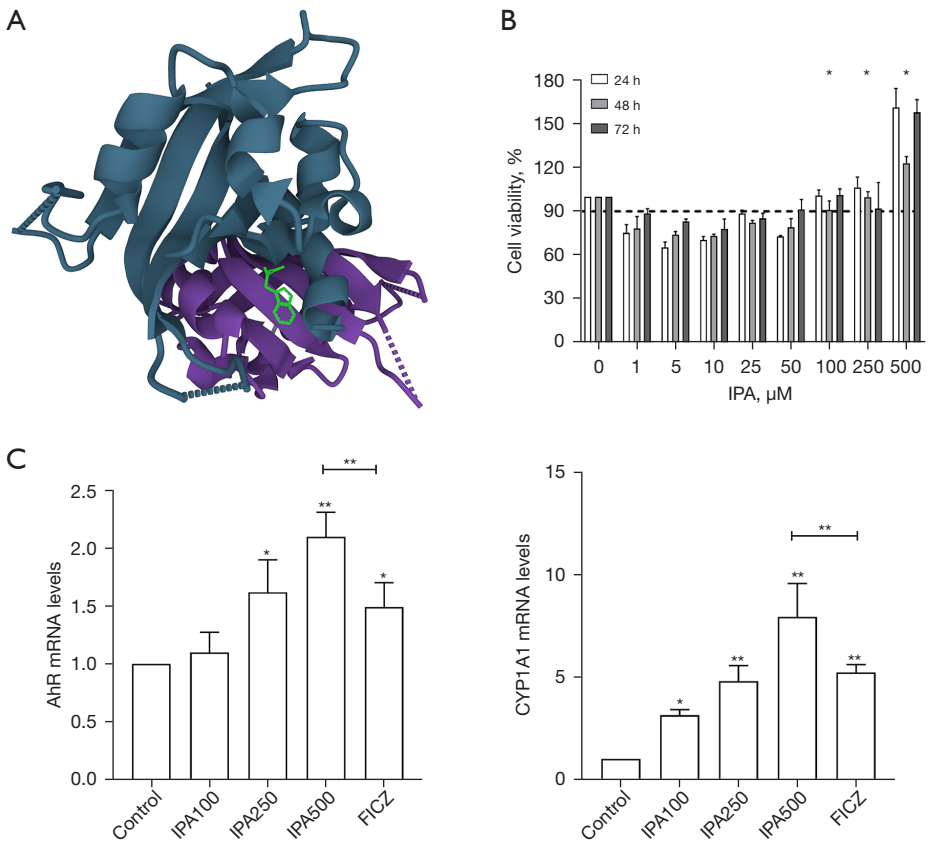

Figure 3 Impact of IPA on PBMCs. (A) Molecular docking of IPA in the AhR ligand-binding domain; (B) cell viability assay after IPA treatment at 0, 1, 5, 10, 25, 50, 100, 250, and 500 μM by CCK-8 assay. The data are presented as the mean ± SD (n=3). *, cell viability (%) >90. (C) RT-PCR analysis of *AhR* mRNA and *CYP1A1* mRNA (n=3). The data are presented as the mean ± SD. *, P<0.05; **, P<0.01 versus control group. IPA, indole-3-pyruvic acid; PBMC, peripheral blood mononuclear cell; AhR, aryl hydrocarbon receptor; CCK-8, Cell Counting Kit-8; RT-PCR, real-time polymerase chain reaction; mRNA, messenger RNA; FICZ, 6-Formylindolo[3,2-b]carbazole; SD, standard deviation.

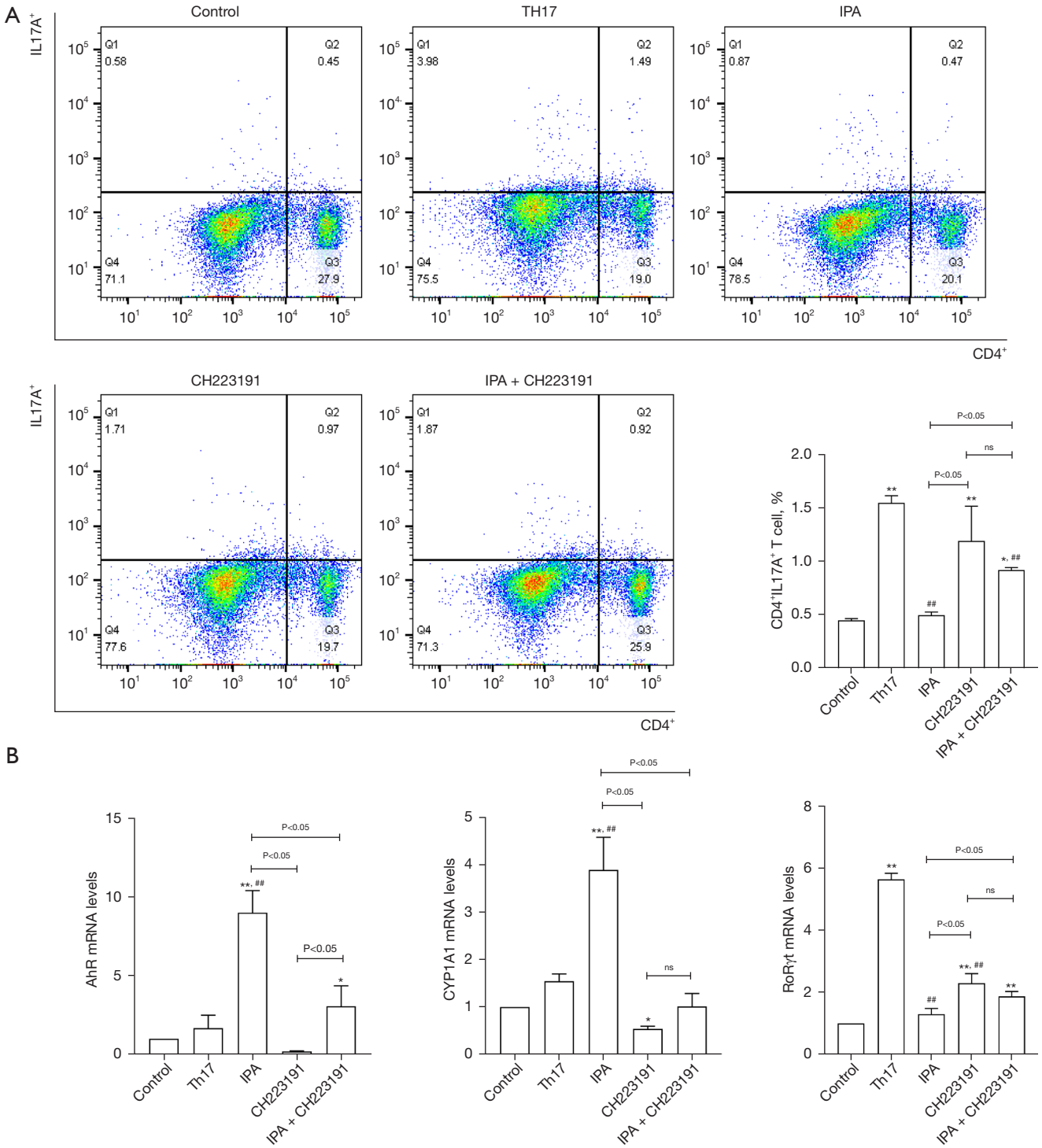

Figure 4 Effect of IPA on the differentiation of Th17 cells through AhR *in vitro*. (A) The effect of IPA on Th17 cell differentiation was detected by flow cytometry assay. The frequency of $CD4^+$ $IL17A^+$ cells was analyzed by flow cytometry (n=3); the data are presented as the mean ± SD. (B) RT-PCR analysis of *AhR* mRNA, *CYP1A1* mRNA, and *RORγt* mRNA (n=3). The data are presented as the mean ± SD. *, P<0.05; **, P<0.01 versus control group; ##, P<0.01 versus Th17 group; ns, P>0.05. IPA, indole-3-pyruvic acid; AhR, aryl hydrocarbon receptor; RT-PCR, real-time polymerase chain reaction; mRNA, messenger RNA; RORγt, Retinoid-related orphan receptor gamma-t; SD, standard deviation.

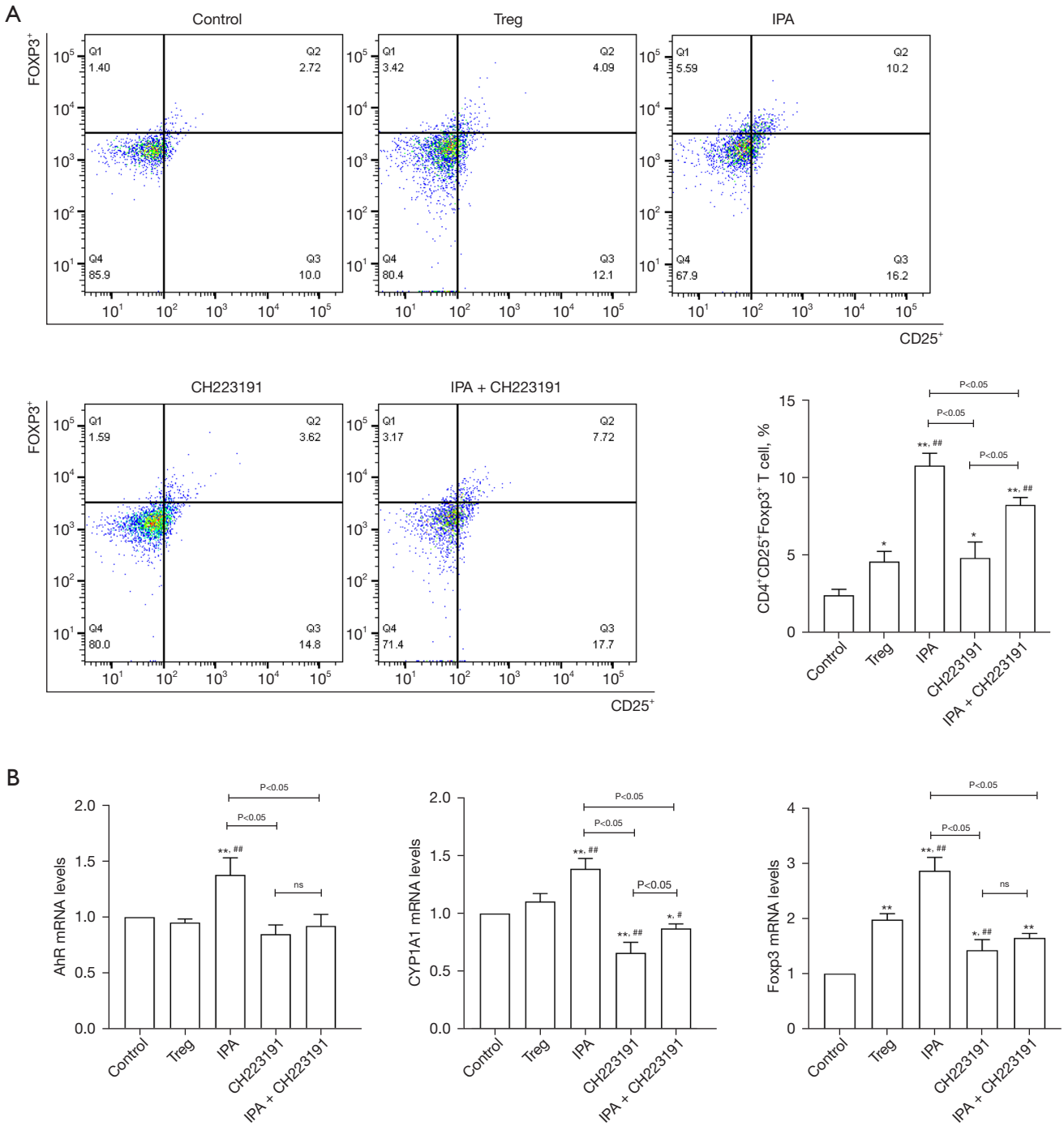

Figure 5 Effect of IPA on the differentiation of Treg cells through AhR *in vitro*. (A) The effect of IPA on Treg cell differentiation was detected by flow cytometry assay. The frequency of $CD4^+CD25^+Foxp3^+$ cells was analyzed by flow cytometry (n=3). The data are presented as the mean ± SD. (B) RT-PCR analysis of *AhR* mRNA, *CYP1A1* mRNA, and *Foxp3* mRNA (n=3). The data are presented as the mean ± SD. *, P<0.05; **, P<0.01 versus control group; #, P<0.05; ##, P<0.01 versus Treg group; ns, P>0.05. IPA, indole-3-pyruvic acid; AhR, aryl hydrocarbon receptor; RT-PCR, real-time polymerase chain reaction; mRNA, messenger RNA; SD, standard deviation.

treatment for CIA. We found that the rats in the CIA group had a rapid immune response to bovine type II collagen and developed arthritis; however, IPA treatment reduced paw swelling and erythema in animals. Histological and radiological manifestations also showed that IPA improved synovial hyperplasia, inflammatory cell infiltration, and bone destruction (*Figure 6A-6C*). The serum IL-1β, TNF-α, and IL-6 levels were the highest in the CIA group; however, the levels of these proinflammatory cytokines decreased significantly after IPA treatment. We also evaluated the levels of Th-related cytokines and found that IPA significantly reduced IL-17A levels. The serum level of IL-10 increased (*Figure 6D*).

CH223191 reversed the effect of IPA in rats with CIA

We co-administered IPA and CH223191 to rats with CIA to estimate the extent of arthritis amelioration by IPA in the animals. The obtained data indicated that the therapeutic effect of IPA on arthritis was significantly reduced by CH223191. CH223191 also reversed the changes in the serum levels of TNF-α, IL-1β, IFN-γ, and IL-10 that were induced by IPA administration (*Figure* 7).

Effect of IPA on the Th17/Treg cell balance in CIA rats

There were no significant differences in the levels of *AhR* mRNA between healthy rats and CIA rats. IPA treatment increased the mRNA expression of *AhR*, but CH223191 treatment significantly reduced these effects. As the target gene of AhR, *CYP1A1* exhibited changes similar to those of the above receptors at the mRNA and protein levels. To determine whether IPA affects the immune balance of RA, we examined the effect of IPA on Th17 and Treg cells in CIA rats after i.p. administration of the drug. Compared with healthy rats, Th17 cells in the spleen of CIA rats were significantly increased, whereas Treg cells were significantly decreased. After IPA treatment, *Foxp3* mRNA expression increased, the CIA-related immune imbalance was reversed, and Treg cells increased significantly, resulting in a low proportion of Th17 cells in the spleen. Although rats treated with IPA exhibited reductions in Th17 cells, animals treated with IPA and CH223191 exhibited increased proportions of Th17 cells and significantly reduced inhibition of *RORγt* mRNA expression by IPA (*Figure 8*).

Discussion

RA is an autoimmune disease accompanied by metabolic changes that alter glucose, lipid, and amino acid levels, affecting glycolysis, the citric acid cycle, the pentose phosphate pathway, the arachidonic acid metabolism pathway, and amino acid metabolism. These metabolic changes may lead to cell proliferation, increased secretion of inflammatory mediators, inflammatory infiltration, and joint damage (24). In this study, we first analyzed the plasma of nonsmoking RA patients and nonsmoking healthy volunteers based on LC-MS metabonomics technology. We can observe that RA affects the pathways of Trp metabolism, steroid hormone biosynthesis, primary bile acid biosynthesis, histidine metabolism, and biosynthesis of unsaturated fatty acids. Among these, the Trp metabolism pathway is the most significantly affected. We further analyzed the differential metabolites in this pathway and screened IPA as a potential biomarker of RA.

Trp can be metabolized by the gut microbiota and probiotics to produce indole derivatives such as indole-3-acetic acid, indole-3-aldehyde, indole-lactic acid, and indole-propionic acid (14). These metabolites can act as AhR ligands to exert their effects (25). AhR is a ligand-inducible transcription factor that can be expressed in immune and epithelial cells (26). Bacteria can metabolize Trp from the diet to produce various indole derivatives, which can activate AhR activity (27). Currently, there are studies suggesting that indole can cross the blood-brain barrier and inhibit pro-inflammatory activity by activating AhR in astrocytes (28). In mouse experiments, the lack of dietary Trp intake or reduced AhR expression led to more severe EAE (experimental autoimmune encephalomyelitis) symptoms. This effect could be reversed by supplementing Trp in control mice. However, EAE symptoms could not be alleviated by Trp supplementation in AhR-/- mice (28).

IPA is a kind of Trp metabolite that can be synthesized through the action of aromatic amino acid transaminase or amino acid oxidase, or produced by some microbes through Trp deamination (29,30). It provides important biochemical substances for cells and exhibits antioxidant properties (31). Previous studies have reported that IPA has the potential to reduce striatal damage after transient forebrain ischemia in rats (32), improve sleep disorders (33), inhibit human anxiety (34), and prevent chronic inflammation in the

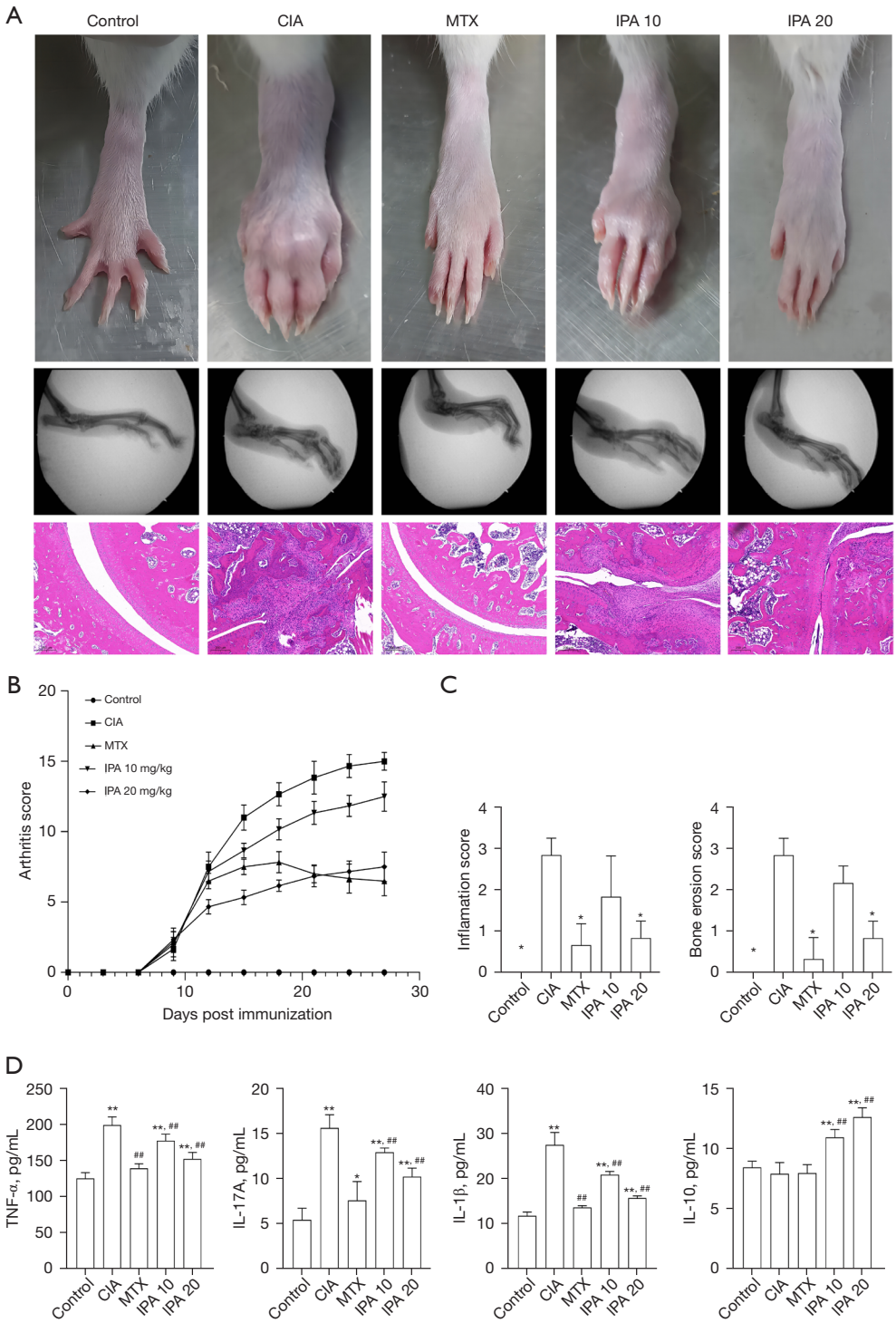

Figure 6 Effect of IPA in rats with CIA. (A) Representative photographs of hind paws, X-ray graph and pathological sections (Ankle joints tissues were stained using hematoxylin and eosin stain, ×150) from each group. (B) Arthritis scores (n=6). The data are presented as mean ± SD. (C) The inflammation score and bone erosion score of pathological sections (n=6). The data are presented as mean ± SD. (D) The levels of TNF-α, IL-1β, IL-17A, and IL-10 in serum were measured using ELISA kits (n=6). The data are presented as mean ± SD. *, P<0.05; **, P<0.01 versus control group; ##, P<0.01 versus the CIA group. IPA, indole-3-pyruvic acid; CIA, collagen-induced arthritis; MTX, methotrexate; ELISA, enzyme-linked immunosorbent assay; SD, standard deviation.

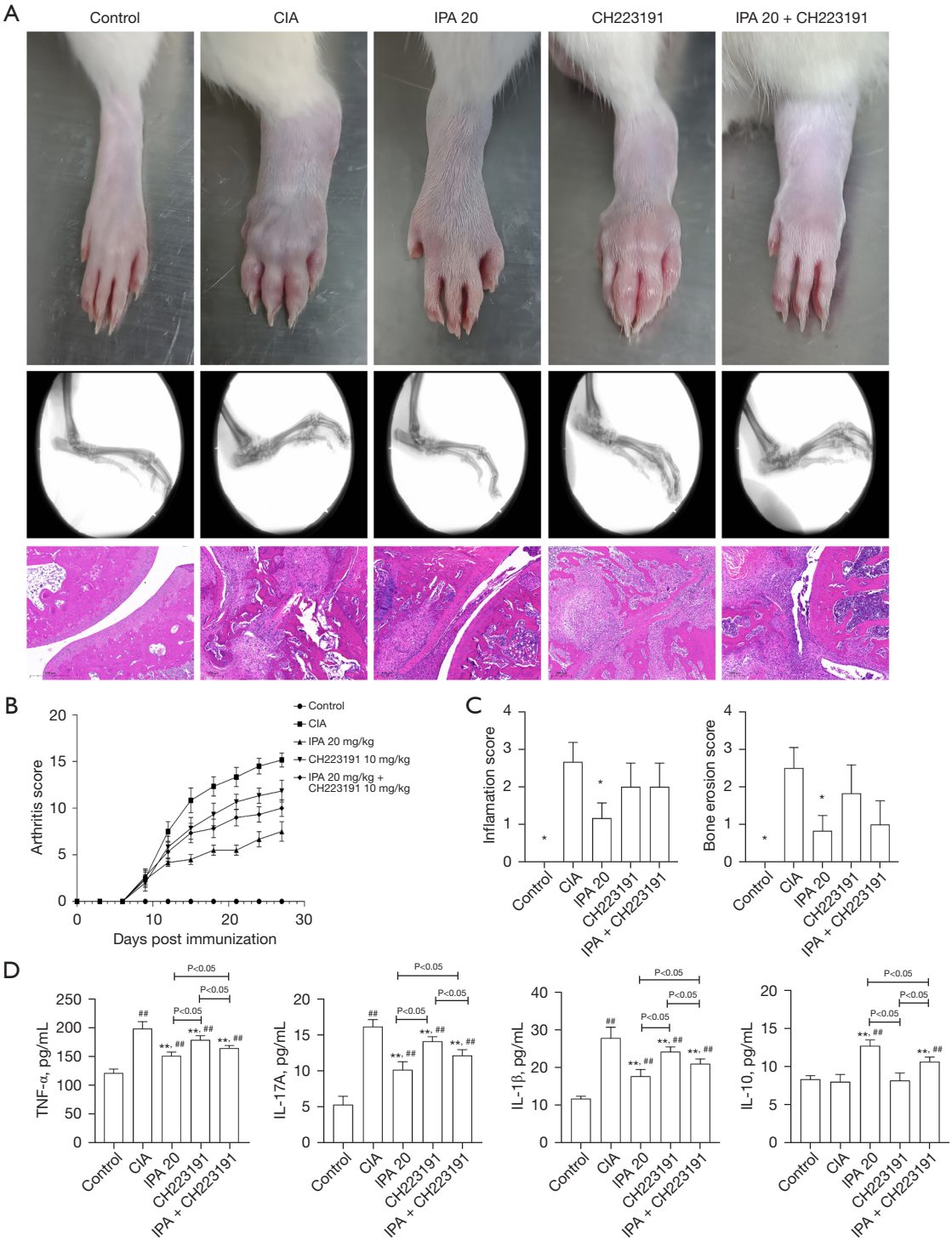

Figure 7 CH223191 reversed the effect of IPA in rats with CIA. (A) Representative photographs of hind paws, X-ray images, and pathological sections (Ankle joints tissues were stained using hematoxylin and eosin stain, ×150) from each group. (B) Arthritis scores. (n=6). The data are presented as mean ± SD (n=6). (C) The inflammation score and bone erosion score of pathological sections (n=6). The data are presented as mean ± SD. (D) The levels of TNF-α, IL-1β, IL-17A, and IL-10 in serum were measured using ELISA kits (n=6). The data are presented as mean ± SD *, P<0.05; **, P<0.01 versus control group; ##, P<0.01 versus the CIA group. IPA, indole-3-pyruvic acid; CIA, collagen-induced arthritis; ELISA, enzyme-linked immunosorbent assay; SD, standard deviation.

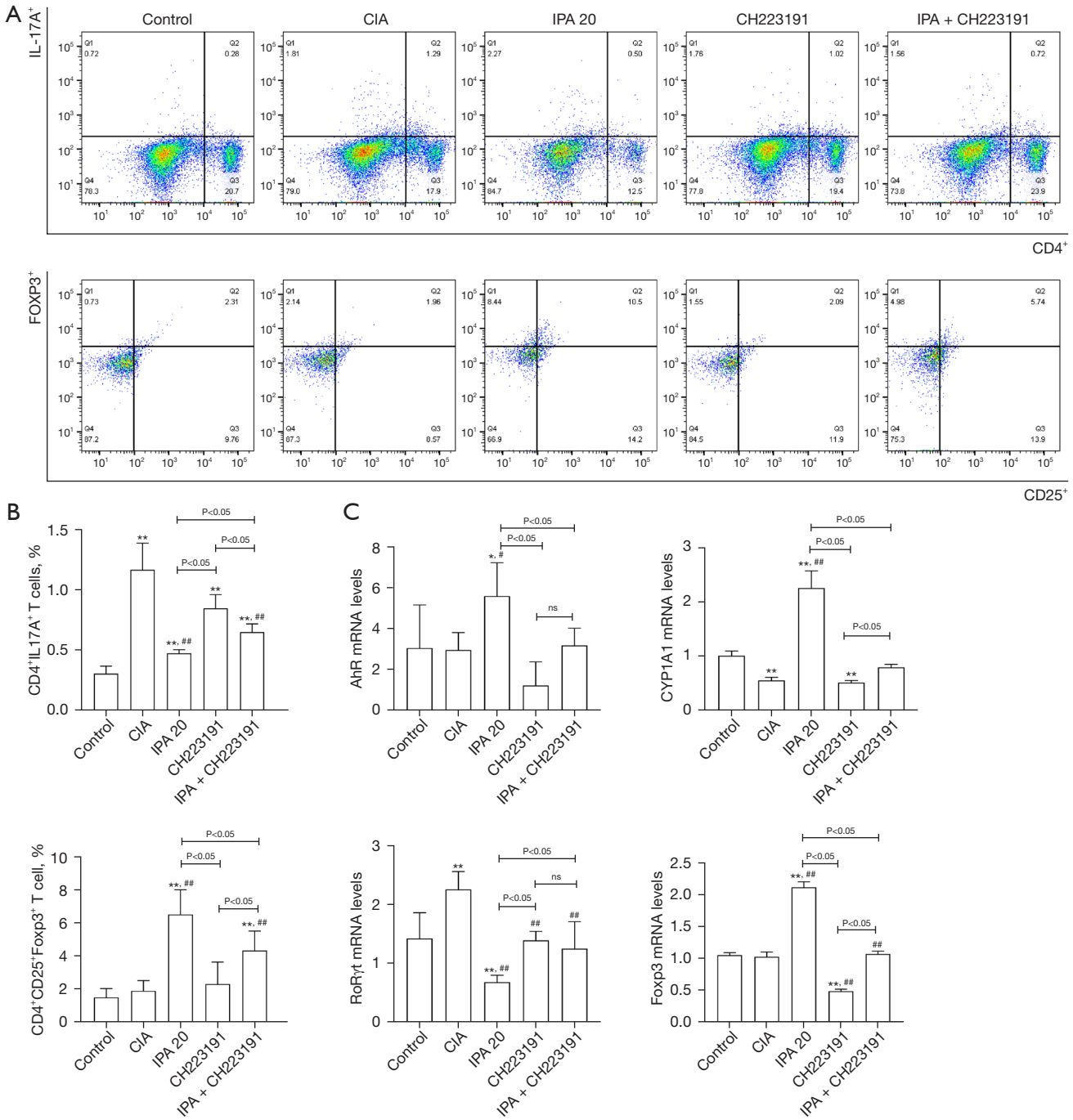

Figure 8 Effect of IPA on the Th17/Treg cell balance in CIA rats. (A) Representative flow cytometry data for the T-cell subsets gated on the $CD4^+$ T cells from the spleens. Representative flow cytometry data for the T-cell subsets gated on the $CD25^+$ T cells from the spleens. (B) The proportion of $CD4^+$ $IL17A^+$ T cells were determined (n=6) and the proportion of $CD4^+CD25^+Foxp3^+$ cells was determined (n=6). The data are presented as the mean ± SD. (C) RT-PCR analysis of *AhR* mRNA, *CYP1A1* mRNA, *RORγt* mRNA, and *Foxp3* mRNA (n=6). The data are presented as the mean ± SD. *, P<0.05; **, P<0.01 versus control group; #, P<0.05 ##, P<0.01 versus CIA group; ns, P>0.05. IPA, indole-3-pyruvic acid; CIA, collagen-induced arthritis; RT-PCR, real-time polymerase cahin reaction; AhR, aryl hydrocarbon receptor; mRNA, messenger RNA; SD, standard deviation.

colon (35). The antioxidant and anti-inflammatory properties of IPA make it potentially useful in the treatment of chronic diseases. As our data showed, the relative expression of IPA was negatively correlated with the DAS28 in patients with RA. When we observed the IPA-treated PBMCs at the condition of the differentiation of Th17 cells, we found that it significantly inhibited the generation of Th17 cells. Previous research has reported that the level of Th17 cells in peripheral blood and IL-17 was positively correlated with DAS28, C-reactive protein (CRP), and erythrocyte sedimentation rate (ESR) (36), which can explain the relationship between IPA and the disease activity.

AhR, a cytoplasmic ligand-activated transcription factor in the basic helical loop (bHLH)/PerARNT-Sim (PAS) superfamily (37), was originally identified as an environmental sensor of exogenous chemicals. Upon ligand binding, AhR translocates to the nucleus and heterodimerizes with the AhR nuclear translocator (ARNT/HIF1β) to promote the effects of AhR-responsive DNA elements in its regulatory regions (e.g., CYP1A1, CYP1A2, and CYP1B1 or AhRR) and the transcription of multiple response genes [with the dioxin response element (DRE) or heterologous response element (XRE)]. AhR has multiple potential functions in the immune system (38). It can regulate a variety of physiological, toxicological, and pharmacological responses. For RA, various natural products can alleviate synovial inflammation and restore immune balance by binding to AhR in both fibroblast-like synoviocytes and T cells, providing new targets and approaches for the treatment of RA (39).

AhR plays a critical role in driving the differentiation of Treg cells (40). AhR signaling directly forms Treg differentiation by regulating the methylation state of Foxp3 promoter. DNA methylation in a gene promoter region is associated with loss of that gene's expression (41). TCDD mediates the partial demethylation of Foxp3 promoter, thereby enhancing the expression of Foxp3; it also mediates the methylation of IL-17 promoter, and reduces the expression of proinflammatory cytokine IL-17 secreted by TH17 cells (42). IPA, a potent AhR agonist (43), can closely combine with AhR and promote its expression. In the current study, IPA upregulated *Foxp3* gene expression and increased Treg cells via an AhR-dependent pathway. Other categories of Trp metabolite in the indole pathway, including indole-3-acetic acid and indole-3-carbinol, are also manifested activation on AhR. Treg cells are the main suppressive cells that maintain tolerance and inhibit autoantigen immunity, characterized by the expression of the transcription factor Foxp3 (44), and are an ideal target for maintaining immune homeostasis and restoring RA antigen-specific tolerance (45). Thus, IPA is more than likely to induce Treg cells and consequently inhibit arthritis through the regulation of AhR.

Proinflammatory cytokines are believed to play a crucial role in the development of CIA by activating immune and inflammatory cells. These cytokines are particularly important in regulating synovitis, as well as cartilage and bone erosion in CIA (46). In this study, oral IPA effectively improved CIA severity and reduced the levels of proinflammatory cytokines and autoantibodies. Notably, IPA treatment decreased the level of IL-17 and increased the level of the anti-inflammatory factor IL-10 in the serum of CIA rats. IL-17 is mainly produced by Th17 cells to activate responding T cells and plays an important role in the inflammation associated with CIA (47). On the other hand, IL-10 is primarily produced by Treg cells and has been shown to inhibit Th17 cell differentiation in the $CD4^+$ T cell population of patients with RA (48). Treg cells play a critical role in immune system regulation by suppressing autoimmune responses and limiting chronic inflammation (49). The findings suggest that the anti-arthritic effect of IPA may be attributed to the restoration of the balance between Th17 and Treg cells. The relationship between Th17 and Treg cells in the development of RA is complex, and maintaining a balance between these two cell types is crucial for ensuring normal immune function and protecting against autoimmune responses.

This study recruited only 14 patients with RA, which may be considered a small sample size. This may be attributed to strict inclusion and exclusion criteria that were developed based on the research design and hypothesis, and in accordance with clear diagnostic criteria. Patients with relatively homogeneous clinical characteristics and demographic similarities were selected from a complex population for the study. Key confounding factors were limited, resulting in a relatively uniform sample that achieved the initial research objectives. However, the reduced sample size may limit the representativeness of the study population, and thus multicenter studies should be conducted to increase the sample size and improve the generalizability of the study results.

In addition, the gut microbiota is a crucial system in the human body that is closely linked to the immune and metabolic systems (50). This study demonstrates that IPA, a Trp metabolite produced by gut microbiota metabolism, can alleviate RA by activating the AhR pathway. This finding

lays the groundwork for further exploration of the effects of gut microbiota metabolites on RA. However, additional experiments are needed to confirm whether the expression level of IPA in the body is influenced by the gut microbiota, which will provide a basis for a better understanding of the role of gut microbiota in the pathogenesis of RA.

Conclusions

In summary, we conclude that IPA may be a protective factor against RA and that IPA can improve the balance of Th17/Treg cells through the AhR pathway, thereby improving CIA.

Acknowledgments

The authors thank the Key Laboratory of Antiinflammatory and Immune Medicine, Ministry of Education, the Center for Scientific Research of Anhui Medical University, and the Center for Scientific Research of The Second Affiliated Hospital of Anhui Medical University for valuable help in the experiment.
Funding: This work was funded by the first batch (2020) of the Key Projects of the Clinical Research Cultivation Plan of the Second Affiliated Hospital of Anhui Medical University (No. 2020LCZD22).

Footnote

Reporting Checklist: The authors have completed the ARRIVE reporting checklist. Available at https://atm.amegroups.com/article/view/10.21037/atm-23-1074/rc

Data Sharing Statement: Available at https://atm.amegroups.com/article/view/10.21037/atm-23-1074/dss

Peer Review File: Available at https://atm.amegroups.com/article/view/10.21037/atm-23-1074/prf

Conflicts of Interest: All authors have completed the ICMJE uniform disclosure form (available at https://atm.amegroups.com/article/view/10.21037/atm-23-1074/coif). All authors report that this work was funded by the first batch (2020) of the Key Projects of the Clinical Research Cultivation Plan of the Second Affiliated Hospital of Anhui Medical University (No. 2020LCZD22). The authors have no other conflicts of interest to declare.

Ethical Statement: The authors are accountable for all aspects of the work in ensuring that questions related to the accuracy or integrity of any part of the work are appropriately investigated and resolved. This study was conducted in accordance with the Declaration of Helsinki (as revised in 2013), and the protocol was approved by the Ethics Committee of The Second Affiliated Hospital of Anhui Medical University (No. YX2021-131). All participants provided informed consent. The animal experiments were performed under a project license (No. PZ-2022-22) granted by Experimental Animal Ethics Committee of the Institute of Clinical Pharmacology of Anhui Medical University, in compliance with Anhui Medical University guidelines for the care and use of animals.

References

1. Smith MH, Berman JR. What Is Rheumatoid Arthritis? JAMA 2022;327:1194.
2. Petrelli F, Mariani FM, Alunno A, et al. Pathogenesis of rheumatoid arthritis: one year in review 2022. Clin Exp Rheumatol 2022;40:475-82.
3. Zhuang Y, Lu W, Chen W, et al. A narrative review of the role of the Notch signaling pathway in rheumatoid arthritis. Ann Transl Med 2022;10:371.
4. Yang P, Qian FY, Zhang MF, et al. Th17 cell pathogenicity and plasticity in rheumatoid arthritis. J Leukoc Biol 2019;106:1233-40.
5. Jiang Q, Yang G, Liu Q, et al. Function and Role of Regulatory T Cells in Rheumatoid Arthritis. Front Immunol 2021;12:626193.
6. Wang W, Shao S, Jiao Z, et al. The Th17/Treg imbalance and cytokine environment in peripheral blood of patients with rheumatoid arthritis. Rheumatol Int 2012;32:887-93.
7. Wang XS, Cao F, Zhang Y, et al. Therapeutic potential of aryl hydrocarbon receptor in autoimmunity.

Inflammopharmacology 2020;28:63-81.
8. Schiering C, Vonk A, Das S, et al. Cytochrome P4501-inhibiting chemicals amplify aryl hydrocarbon receptor activation and IL-22 production in T helper 17 cells. Biochem Pharmacol 2018;151:47-58.
9. Cheng L, Qian L, Xu ZZ, et al. Aromatic hydrocarbon receptor provides a link between smoking and rheumatoid arthritis in peripheral blood mononuclear cells. Clin Exp Rheumatol 2019;37:445-9.
10. Quintana FJ, Basso AS, Iglesias AH, et al. Control of T(reg) and T(H)17 cell differentiation by the aryl hydrocarbon receptor. Nature 2008;453:65-71.
11. Xi X, Ye Q, Fan D, et al. Polycyclic Aromatic Hydrocarbons Affect Rheumatoid Arthritis Pathogenesis via Aryl Hydrocarbon Receptor. Front Immunol 2022;13:797815.
12. Lavelle A, Sokol H. Gut microbiota-derived metabolites as key actors in inflammatory bowel disease. Nat Rev Gastroenterol Hepatol 2020;17:223-37.
13. Ghiboub M, Verburgt CM, Sovran B, et al. Nutritional Therapy to Modulate Tryptophan Metabolism and Aryl Hydrocarbon-Receptor Signaling Activation in Human Diseases. Nutrients 2020;12:2846.
14. Roager HM, Licht TR. Microbial tryptophan catabolites in health and disease. Nat Commun 2018;9:3294.
15. Noack M, Miossec P. Th17 and regulatory T cell balance in autoimmune and inflammatory diseases. Autoimmun Rev 2014;13:668-77.
16. Sonowal R, Swimm A, Sahoo A, et al. Indoles from commensal bacteria extend healthspan. Proc Natl Acad Sci U S A 2017;114:E7506-15.
17. Aletaha D, Neogi T, Silman AJ, et al. 2010 Rheumatoid arthritis classification criteria: an American College of Rheumatology/European League Against Rheumatism collaborative initiative. Arthritis Rheum 2010;62:2569-81.
18. Shi Y, Zhang J, Mao Z, et al. Extracellular Vesicles From Gastric Cancer Cells Induce PD-L1 Expression on Neutrophils to Suppress T-Cell Immunity. Front Oncol 2020;10:629.
19. Biagini G, Pich EM, Carani C, et al. Indole-pyruvic acid, a tryptophan ketoanalogue, antagonizes the endocrine but not the behavioral effects of repeated stress in a model of depression. Biol Psychiatry 1993;33:712-9.
20. Li X, Lu C, Fan D, et al. Human Umbilical Mesenchymal Stem Cells Display Therapeutic Potential in Rheumatoid Arthritis by Regulating Interactions Between Immunity and Gut Microbiota via the Aryl Hydrocarbon Receptor. Front Cell Dev Biol 2020;8:131.
21. Cao W, Lu J, Li L, et al. Activation of the Aryl Hydrocarbon Receptor Ameliorates Acute Rejection of Rat Liver Transplantation by Regulating Treg Proliferation and PD-1 Expression. Transplantation 2022;106:2172-81.
22. Morris GM, Huey R, Olson AJ. Using AutoDock for ligand-receptor docking. Curr Protoc Bioinformatics 2008;Chapter 8:Unit 8.14.
23. Wang Y, Bryant SH, Cheng T, et al. PubChem BioAssay: 2017 update. Nucleic Acids Res 2017;45:D955-63.
24. Xu L, Chang C, Jiang P, et al. Metabolomics in rheumatoid arthritis: Advances and review. Front Immunol 2022;13:961708.
25. Korecka A, Dona A, Lahiri S, et al. Bidirectional communication between the Aryl hydrocarbon Receptor (AhR) and the microbiome tunes host metabolism. NPJ Biofilms Microbiomes 2016;2:16014.
26. Bersten DC, Sullivan AE, Peet DJ, et al. bHLH-PAS proteins in cancer. Nat Rev Cancer 2013;13:827-41.
27. Zelante T, Iannitti RG, Cunha C, et al. Tryptophan catabolites from microbiota engage aryl hydrocarbon receptor and balance mucosal reactivity via interleukin-22. Immunity 2013;39:372-85.
28. Rothhammer V, Mascanfroni ID, Bunse L, et al. Type I interferons and microbial metabolites of tryptophan modulate astrocyte activity and central nervous system inflammation via the aryl hydrocarbon receptor. Nat Med 2016;22:586-97.
29. Krishnamurthi VS, Buckley PJ, Duerre JA. Pigment formation from L-tryptophan by a particulate fraction from an Achromobacter species. Arch Biochem Biophys 1969;130:636-45.
30. McGettrick AF, Corcoran SE, Barry PJ, et al. Trypanosoma brucei metabolite indolepyruvate decreases HIF-1α and glycolysis in macrophages as a mechanism of innate immune evasion. Proc Natl Acad Sci U S A 2016;113:E7778-87.
31. Politi V, D'Alessio S, Di Stazio G, et al. Antioxidant properties of indole-3-pyruvic acid. Adv Exp Med Biol 1996;398:291-8.
32. Zoli M, Merlo Pich E, Ferraguti F, et al. Indole-pyruvic acid treatment reduces damage in striatum but not in hippocampus after transient forebrain ischemia in the rat. Neurochem Int 1993;23:139-48.
33. Silvestri R, Mento G, Raffaele M, et al. Indole-3-pyruvic acid as a possible hypnotic agent in insomniac subjects. J Int Med Res 1991;19:403-9.
34. Politi V, De Luca G, Gallai V, et al. Clinical experiences with the use of indole-3-pyruvic acid. Adv Exp Med Biol

1999;467:227-32.
35. Aoki R, Aoki-Yoshida A, Suzuki C, et al. Indole-3-Pyruvic Acid, an Aryl Hydrocarbon Receptor Activator, Suppresses Experimental Colitis in Mice. J Immunol 2018;201:3683-93.
36. Chen DY, Chen YM, Chen HH, et al. Increasing levels of circulating Th17 cells and interleukin-17 in rheumatoid arthritis patients with an inadequate response to anti-TNF-α therapy. Arthritis Res Ther 2011;13:R126.
37. Schulte KW, Green E, Wilz A, et al. Structural Basis for Aryl Hydrocarbon Receptor-Mediated Gene Activation. Structure 2017;25:1025-1033.e3.
38. Stockinger B, Di Meglio P, Gialitakis M, et al. The aryl hydrocarbon receptor: multitasking in the immune system. Annu Rev Immunol 2014;32:403-32.
39. Hui W, Dai Y. Therapeutic potential of aryl hydrocarbon receptor ligands derived from natural products in rheumatoid arthritis. Basic Clin Pharmacol Toxicol 2020;126:469-74.
40. Mezrich JD, Fechner JH, Zhang X, et al. An interaction between kynurenine and the aryl hydrocarbon receptor can generate regulatory T cells. J Immunol 2010;185:3190-8.
41. Pot C. Aryl hydrocarbon receptor controls regulatory CD4+ T cell function. Swiss Med Wkly 2012;142:w13592.
42. Singh NP, Singh UP, Singh B, et al. Activation of aryl hydrocarbon receptor (AhR) leads to reciprocal epigenetic regulation of FoxP3 and IL-17 expression and amelioration of experimental colitis. PLoS One 2011;6:e23522.
43. Vrzalová A, Pečinková P, Illés P, et al. Mixture Effects of Tryptophan Intestinal Microbial Metabolites on Aryl Hydrocarbon Receptor Activity. Int J Mol Sci 2022;23:10825.
44. Moser M, Leo O. Key concepts in immunology. Vaccine 2010;28 Suppl 3:C2-13.
45. Rezaei Kahmini F, Shahgaldi S, Azimi M, et al. Emerging therapeutic potential of regulatory T (Treg) cells for rheumatoid arthritis: New insights and challenges. Int Immunopharmacol 2022;108:108858.
46. McInnes IB, Schett G. Cytokines in the pathogenesis of rheumatoid arthritis. Nat Rev Immunol 2007;7:429-42.
47. Wen T, Li Y, Wu M, et al. Therapeutic effects of a novel tylophorine analog, NK-007, on collagen-induced arthritis through suppressing tumor necrosis factor α production and Th17 cell differentiation. Arthritis Rheum 2012;64:2896-906.
48. Heo YJ, Joo YB, Oh HJ, et al. IL-10 suppresses Th17 cells and promotes regulatory T cells in the CD4+ T cell population of rheumatoid arthritis patients. Immunol Lett 2010;127:150-6.
49. Fontenot JD, Gavin MA, Rudensky AY. Foxp3 programs the development and function of CD4+CD25+ regulatory T cells. Nat Immunol 2003;4:330-6.
50. Zhang M, Shi M, Fan M, et al. Comparative Analysis of Gut Microbiota Changes in Pere David's Deer Populations in Beijing Milu Park and Shishou, Hubei Province in China. Front Microbiol 2018;9:1258.

Cite this article as: Huang T, Cheng L, Jiang Y, Zhang L, Qian L. Indole-3-pyruvic acid alleviates rheumatoid arthritis via the aryl hydrocarbon receptor pathway. Ann Transl Med 2023;11(5):213. doi: 10.21037/atm-23-1074

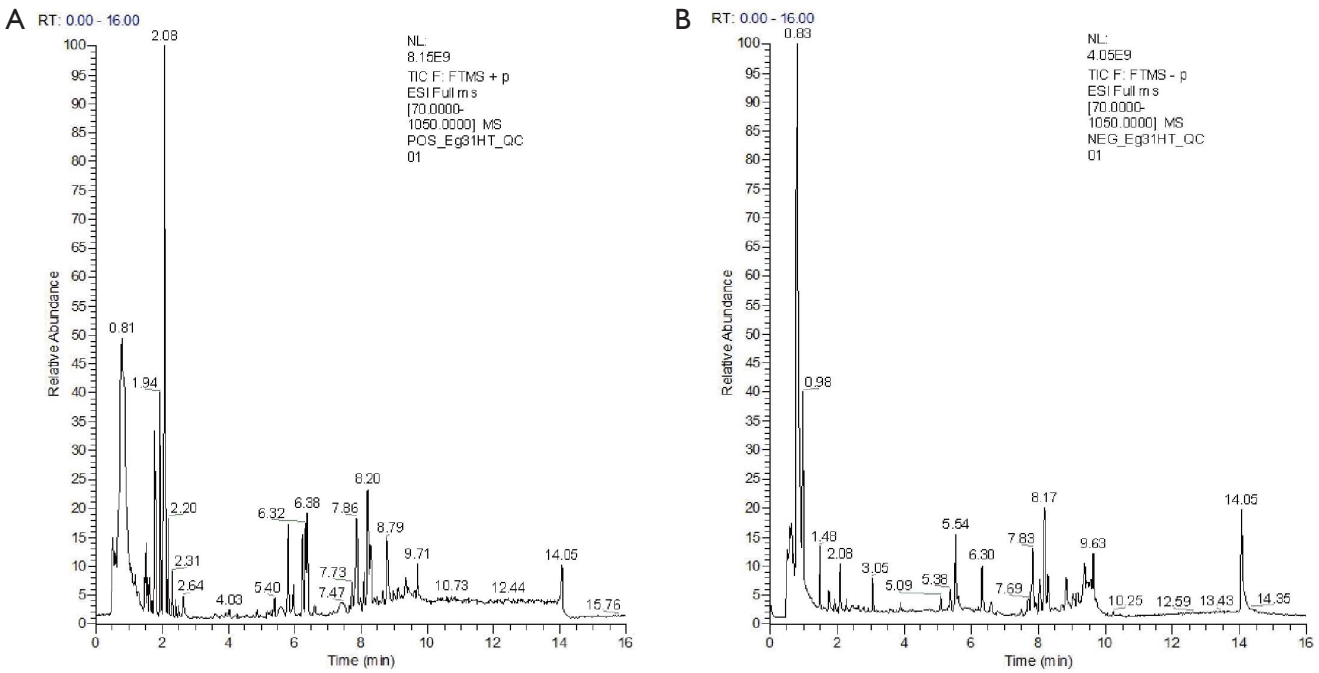

Figure S1 Total ion chromatograms. (A) ESI(+) total ion chromatograms; (B) ESI(–) total ion chromatograms. ESI, Electrospray ionization.

https://dx.doi.org/10.21037/atm-23-1074

Table S1 Mobile phases and gradient elution

Time (min)	Flow rate (mL/min)	Solvent A (%)	Solvent B (%)
0	0.4	100	0
0.1	0.4	95	5
2	0.4	75	25
9	0.4	0	100
13	0.4	0	100
13.1	0.4	100	0
16	0.4	100	0

Table S2 Mass spectrometry parameters

Description	Parameters
Scan type (m/z)	70–1,050
Sheath gas flow rate (arb)	40
Aux gas flow rate (arb)	10
Heater temp (℃)	400
Capillary temp (℃)	320
Spray voltage(+) (V)	3500
Spray voltage(–) (V)	–2,800
S-lens radio frequency level (%)	50
Normalized collision energy (eV)	20, 40, 60
Resolution (Full MS)	70,000
Resolution (MS^2)	17,500

MS, mass spectrometer.

https://dx.doi.org/10.21037/atm-23-1074